

Electronic Supplementary Information (ESI)

Photo-Switchable Smart Superhydrophobic Surface with Controllable Superwettability

Xiaoyan Yang, Haibao Jin, Xinfeng Tao, Binbin Xu and Shaoliang Lin*

Shanghai Key Laboratory of Advanced Polymeric Materials
Key Laboratory for Ultrafine Materials of Ministry of Education
School of Materials Science and Engineering
East China University of Science and Technology
130 Meilong Road, Shanghai, 200237, P. R. China
* Corresponding author: slin@ecust.edu.cn (S. Lin)

Table of Contents

1. Characterization of P4VP- <i>b</i> -PAzoMA.....	3
2. Influence of the concentration of polymer solution on superhydrophobic surface.....	4
3. XPS spectrum of the azopolymer film.	5
4. SEM images and wettability investigation of micropatterns coated with SiO ₂ NPs.	6
5. UV/Vis spectra of the azopolymer film.....	7
6. Change of film color before and after exposure to UV/Vis light.	8
7. DSC characterization of P4VP- <i>b</i> -PAzoMA.	9
8. SEM images of reversible superhydrophobic micropatterns.	10
9. The water adhesion ability on the superhydrophobic azopolymer film.....	11
10. SEM image of azopolymer film after the UV irradiation for 30 min.	12
11. Photoinduced changes of water adhesion ability on unmodified micropatterns.	13
12. Typical SEM images of lotus-leaf-like structure irradiated by LPL with different time.....	14
13. SEM image of superhydrophobic micropatterns after the LPL irradiation for 3 h.	14
14. SEM image of unmodified micropatterns after LPL irradiation and the corresponding wettability.....	15

1. Characterization of P4VP-*b*-PAzoMA.

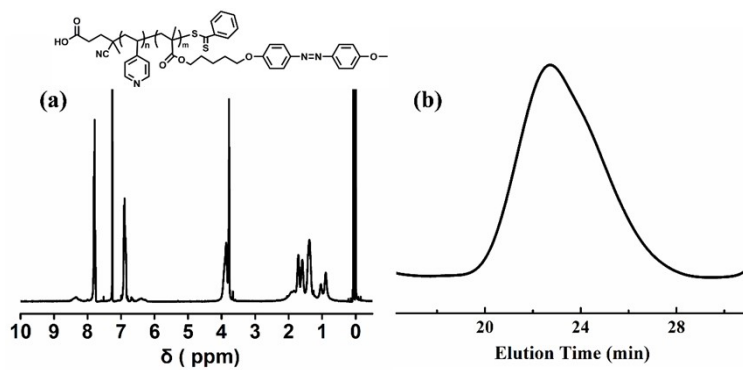


Fig. S1 (a) ^1H NMR spectrum and (b) GPC curve of P4VP-*b*-PAzoMA.

2. Influence of the concentration of polymer solution on superhydrophobic surface.

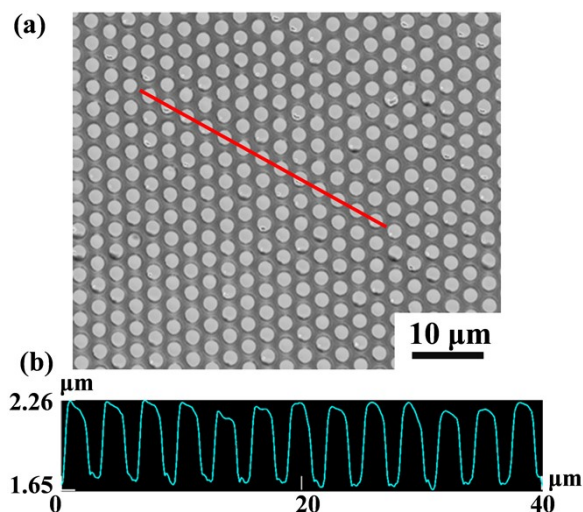


Fig. S2 Confocal laser scanning microscopy image of micro-arrayed film obtained with polymer concentration of 5 mg/mL (a), and the corresponding height profile (b).

When the concentration of the polymer solution is too low (<5 mg/ml), the thickness of the polymer film is only few hundred nanometers (Figure S2), which is too thin to exfoliate the superhydrophobic surface from the substrate. When the solution concentration is too high (>15 mg/ml), the poor solubility results in unevenness of the obtained superhydrophobic surface of the polymer film. Therefore, the optimum polymer concentration is 10 mg/ml.

3. XPS spectrum of the azo-polymer film.

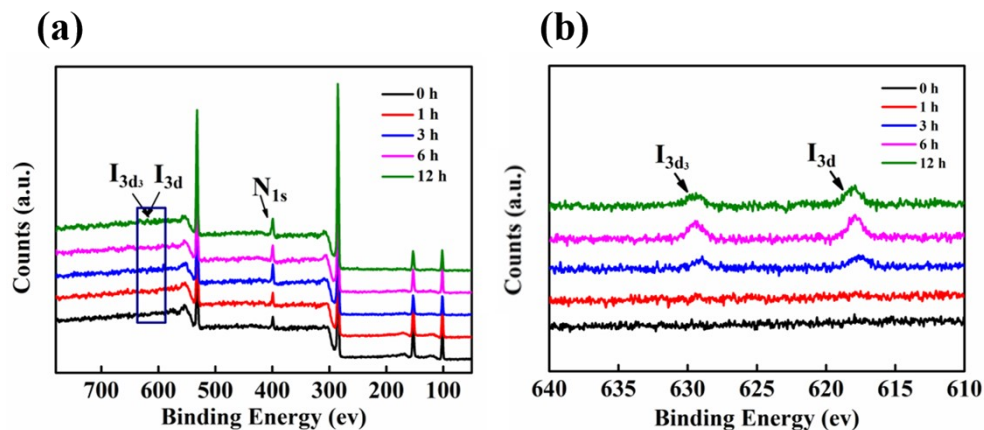


Fig. S3 XPS was used to trace the quaternization degree of the azopolymer film. (a) Full-scan XPS spectrum under different time. (b) Curve-fitted XPS spectrum of the Iodine 3d peaks.

The emergence of two peaks at 618 eV and 630 eV which can be assigned to iodine 3d and 3d₃ electrons (Fig. S3b) could corroborate the occurrence of quaternization reaction. The degree of crosslinking can be analyzed semi-quantitatively according to the integration of the peaks. Notably, the peaks at 6 h and 12 h are almost the same, demonstrating that optimum crosslinking time is 6 h.

4. SEM images and wettability investigation of micropatterns coated with SiO₂ NPs.

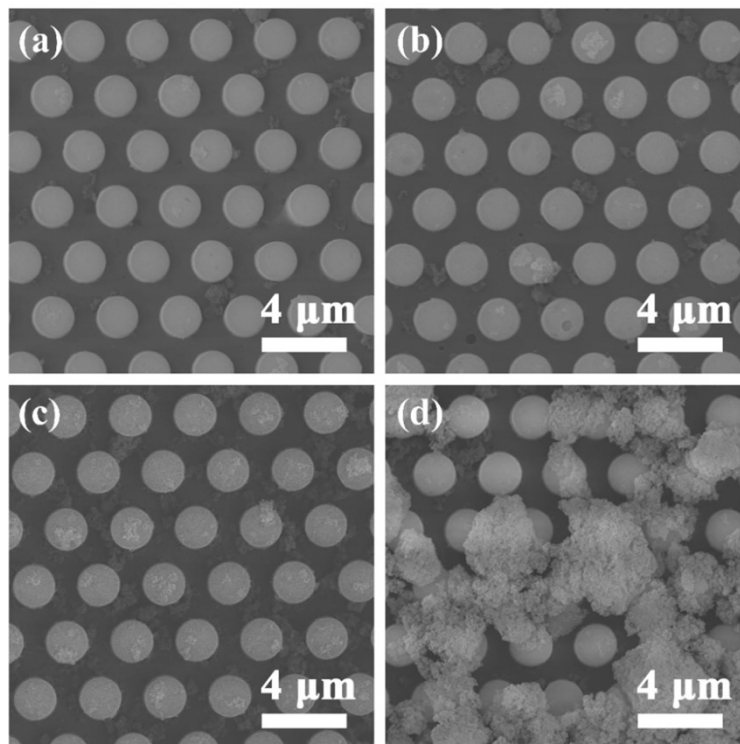


Fig. S4 SEM images of micropatterns coated with silica solution with different concentrations. (a) 0.5%; (b) 1%; (c) 2%; (d) 4%.

Table. S1 Wetting properties of as-prepared superhydrophobic surfaces for different silica concentrations.

Silica Concentration (%)	WCA (°)	WSA (°)
0	144	/
0.5	146	/
1	149	20
2	154	8
4	157	1

5. UV/Vis spectra of the azopolymer film.

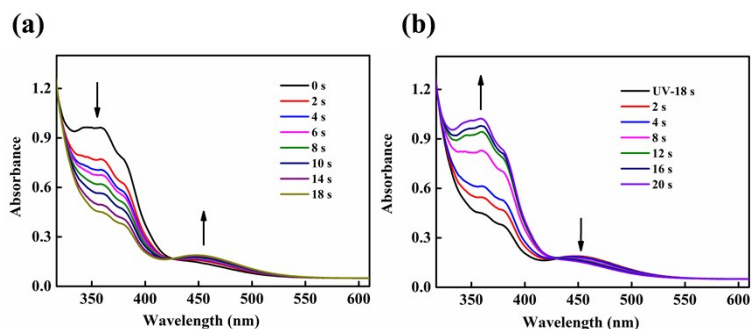


Fig. S5 UV–Vis absorption spectra of the azopolymer film under UV light irradiation (a) and visible light irradiation (b).

There existed two peaks in the UV–vis absorption spectra at approximately 365 nm and 450 nm, corresponding to $\pi\text{-}\pi^*$ and $n\text{-}\pi^*$ transitions of the fluorine-containing azobenzene derivative moieties. Upon UV irradiation, an evident decrease of $\pi\text{-}\pi^*$ absorption at 365 nm and an increase of $n\text{-}\pi^*$ absorption at 450 nm were observed, indicating photoisomerization from the trans to cis isomer of the azobenzene moiety. Further irradiation with visible light caused an increase of $\pi\text{-}\pi^*$ absorption and a decrease of $n\text{-}\pi^*$ absorption, accompanied by the cis to trans conversion of the azobenzene groups.

6. Change of film color before and after exposure to UV/Vis light.

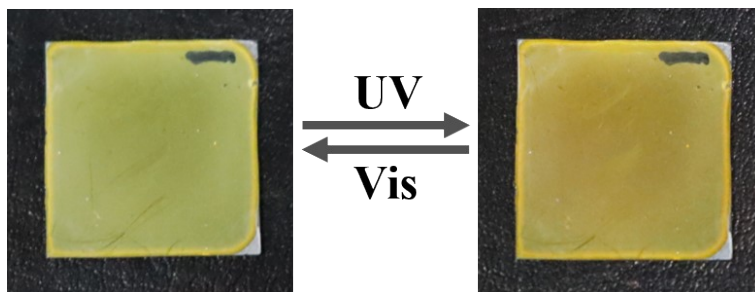


Fig. S6 Photographs of the azo-polymer film before and after exposure to UV and visible light.

7. DSC characterization of P4VP-*b*-PAzoMA.

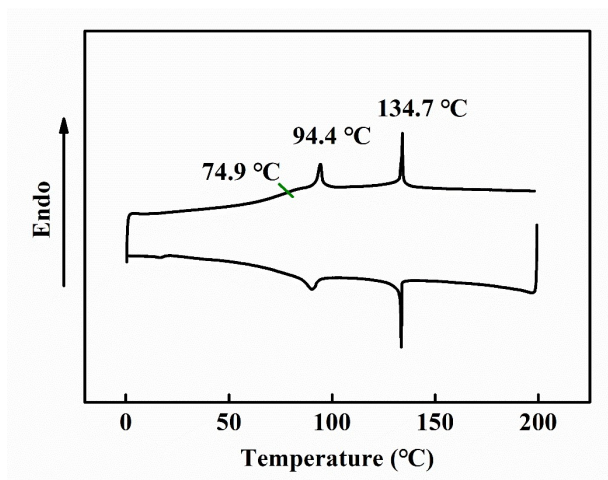


Fig. S7 DSC curve of P4VP-*b*-PAzoMA.

8. SEM images of reversible superhydrophobic micropatterns.

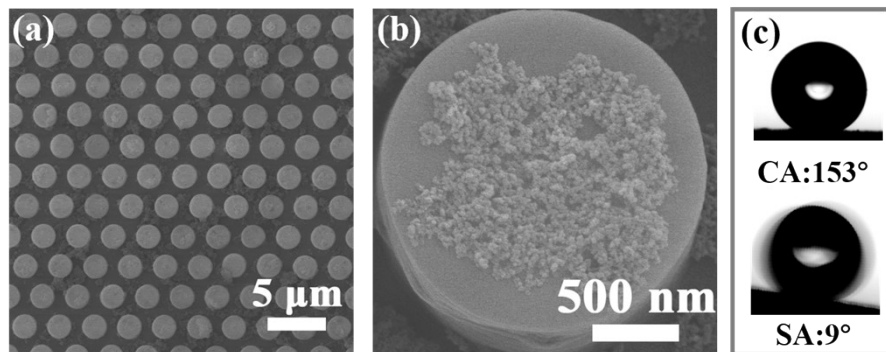


Fig. S8 (a-b) SEM images of micropattern after several times of reversible three-phase-transition; (c) static angle (up) and rolling angle (bottom) of water droplets on the array.

9. The water adhesion ability on the superhydrophobic azopolymer film.

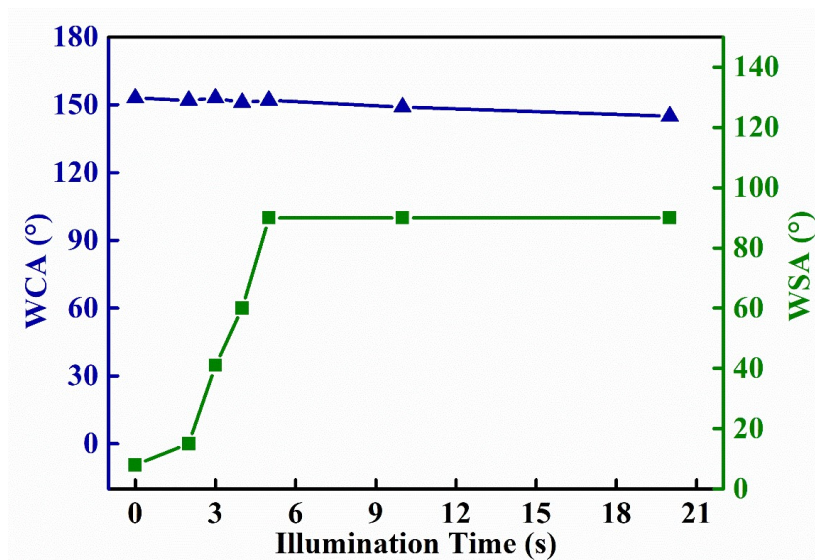


Fig. S9 The water adhesion ability on the superhydrophobic film based on the photomanipulation affect: the variation curves of contact angle (blue line) and sliding angle (green line).

10. SEM image of azopolymer film after the UV irradiation for 30 min.

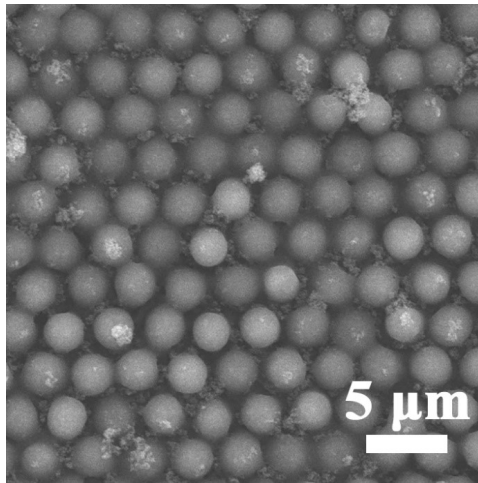


Fig. S10 SEM image of the azopolymer film after the UV irradiation for 30 min, indicating the destroy of the surface microstructure.

11. Photoinduced changes of water adhesion ability on unmodified micropatterns.

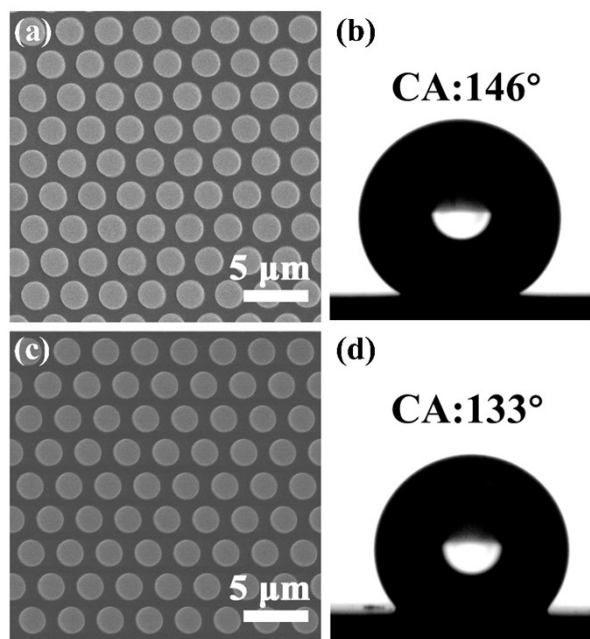


Fig. S11 Photoinduced changes of water adhesion ability on unmodified micropattern. (a) SEM image before UV irradiation; (b) the corresponding static angle; (c) SEM image after UV irradiation for 20 s; (d) the corresponding static angle. The results demonstrate an obvious wetting change induced by UV irradiation.

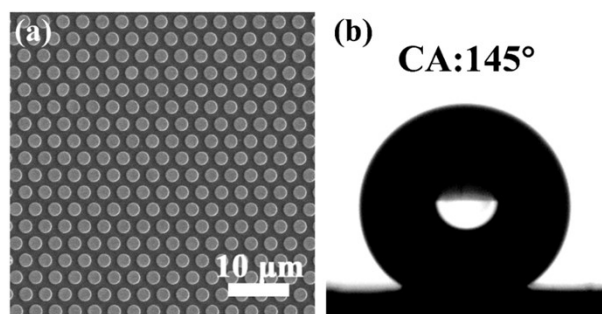


Fig. S12 (a) SEM image of unmodified micropattern after several times of reversible UV/Vis transition; (b) the corresponding static angle.

12. Typical SEM images of lotus-leaf-like structure irradiated by LPL with different time.

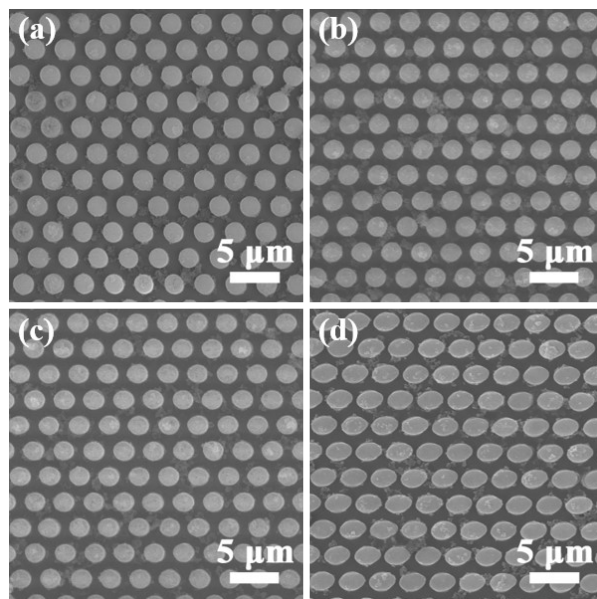


Fig. S13 Typical SEM images of lotus-leaf-like structure irradiated by LPL for different time: (a) 0 min, (b) 5 min, (c) 10 min, (d) 20 min.

13. SEM image of superhydrophobic micropatterns after the LPL irradiation for 3 h.

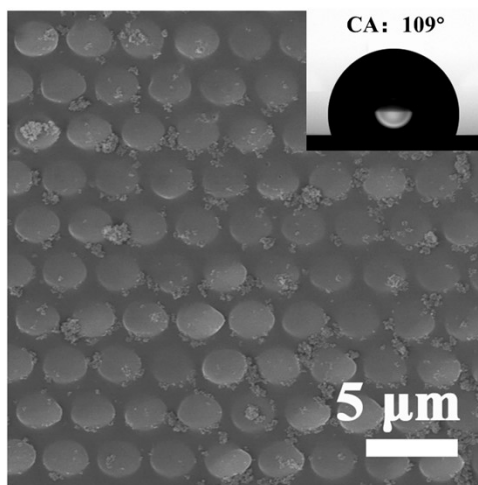


Fig. S14 SEM image of lotus-leaf inspired micropattern irradiated by LPL for 3 h, the inset is the corresponding static angle.

14. SEM image of unmodified micropatterns after LPL irradiation and the corresponding wettability.

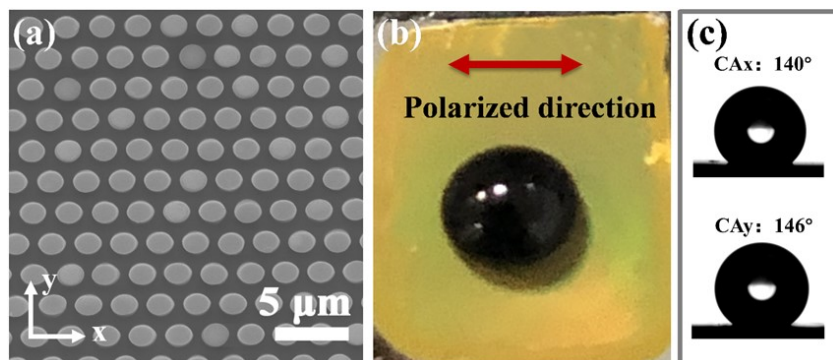


Fig. S15 (a) SEM image of microarray after LPL irradiation for 20 min; (b) Digital image of a colored water droplet shape placed on the sample; (c) CA for different directions. CA_x (up) is perpendicular to the elongated direction, CA_y (bottom) is paralleled to the elongated direction.

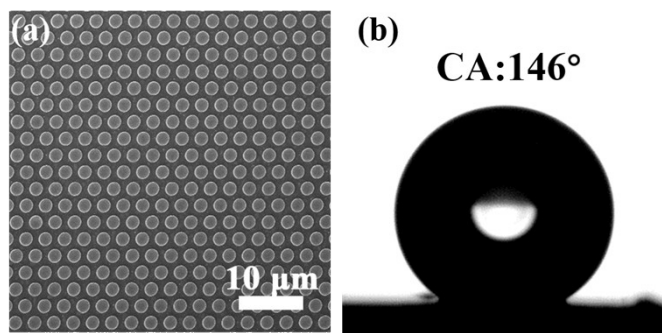


Fig. S16 SEM large-area image of unmodified micropattern after several times of reversible deformation/recovery transition (a), and corresponding static angle (b).